

62

Reprinted from

## Dislocations and Fault Surfaces in Synthetic Quartz

A. R. LANG

*H. H. Wills Physics Laboratory, University of Bristol, Royal Fort, Bristol, England*

AND

V. F. MIUSCOV

*Institute of Crystallography, Academy of Sciences of USSR, Moscow B-333, USSR*

(Received 5 January 1967)

Defects in a rather perfect synthetic quartz crystal have been surveyed by x-ray topography. Etching behavior and stress birefringence were also studied. The crystal, grown from a *z*-plate seed, contained Na and Al in concentrations of 50 ppm by weight. The crystal had grown in the *c* direction with low dislocation density ( $\sim 3000$  lines  $\text{cm}^{-2}$ ). The majority of dislocations made about  $10^\circ$  with the *c* axis, only 15% had Burgers vectors with a *c*-axis component. Cellular growth had developed as growth in the *c* direction proceeded. The cell walls were identified with fault surfaces made visible by diffraction contrast. These surfaces were inclined at fairly small angles with  $[0001]$  and their intersections with (0001) formed an irregular polygonal network. Dislocations congregated in or near the fault surfaces in the later stages of growth. The fault surfaces outcropped at the grooves between protuberances on the rough external crystal surface of mean orientation (0001). The presence of fault fringes indicates impurity segregation in the cell walls: the fringe contrast could arise from a layer a few microns thick with a lattice parameter a few parts in  $10^6$  different from that of surrounding material.

### 1. INTRODUCTION

Alpha quartz is one of the fairly few crystals known to behave as perfect or almost perfect throughout large volumes, when diffracting x rays. Hence, with it one may examine the ways in which perfect-crystal diffraction behavior is modified by the presence of occasional lattice defects which, individually, produce diffraction contrast on x-ray topographs. On the more practical side, one may study the distribution of these defects in the interior of large specimens, with the aim of relating the nature and distribution of such defects to the growth history of the crystal and, possibly, to various properties of the crystal which are of physical and technical interest. Techniques for growing large crystals of quartz are well established<sup>1</sup> and derive from the hydrothermal synthesis experiments of Spezia more than fifty years ago.<sup>2</sup> The art of producing large crystals

of quartz hydrothermally antedates that of producing large semiconductor crystals from the melt, but the latter have now outstripped the former as regards the level of lattice perfection attainable. However, a strong interest attached to synthetic quartz, but lacking in the case of semiconductor crystals, is the existence of large natural quartz crystals possessing many variations in purity and perfection. Comparison of these natural products with laboratory attempts to simulate or improve upon them may throw light on geological as well as physical problems. Moreover, since the quartz structure is much less simple than the diamond structure, a greater variety of lattice imperfections might be expected in the former. X-ray topography confirms this expectation, particularly with respect to types of sheet defects, or "fault surfaces," which commonly occur in natural quartz.<sup>3-5</sup>

An informative recent study of defects in synthetic

<sup>1</sup> A. A. Ballman and R. A. Laudise, in *The Art and Science of Growing Crystals*, J. J. Gilman, Ed. (John Wiley & Sons, Inc., New York, 1963), p. 231.

<sup>2</sup> For a review of early work on growing quartz, see C. S. Brown *et al.*, *Mineral. Mag.* **29**, 858 (1952).

<sup>3</sup> A. R. Lang, *J. Appl. Phys.* **30**, 1748 (1959).

<sup>4</sup> N. Kato and A. R. Lang, *Acta Cryst.* **12**, 787 (1959).

<sup>5</sup> A. R. Lang, in *Proceedings of the International Conference on Crystal Growth, Boston, 1966* (Pergamon Press, Ltd., London, 1967), p. 833.

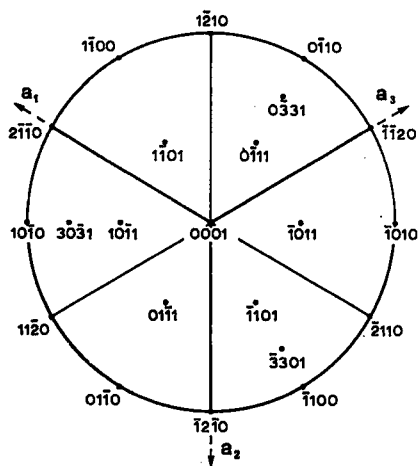


FIG. 1. Stereographic projection on basal plane of quartz showing poles of important Bragg-reflecting planes.

quartz by Spencer and Haruta<sup>6</sup> includes x-ray topographic observations on linear defects which they cautiously identify as dislocations. In the present work we have applied high-resolution topographic methods to the study of these linear defects, and we confirm that they are indeed dislocations. This we assert on the basis of the variation of their visibility in various Bragg reflections, the fine structure of their images, and the similarity of the images to known dislocation images in other crystals. We have also studied fault surfaces. In synthetic quartz there occur types of fault surface rather different from those encountered in natural quartz. We have been able to relate the configuration of fault surfaces to the mode of growth of the crystals and to certain features on the crystal surfaces.

## 2. EXPERIMENTAL METHOD

Figure 1 is a stereographic projection on the basal plane of quartz showing the poles of planes whose Bragg reflections we commonly use in x-ray topographic studies of this crystal. Some of these planes coincide with important faces on natural quartz. Very important are the major rhombohedron,  $r$ ,  $\{10\bar{1}1\}$ , the minor rhombohedron,  $z$ ,  $\{\bar{1}011\}$  and the prism,  $m$ ,  $\{10\bar{1}0\}$ . (Faces of the form  $M$ ,  $\{30\bar{3}1\}$ , may sometimes occur naturally as narrow bevels between the  $m$  and  $r$  faces in the same zone. The forms  $a$ ,  $\{11\bar{2}0\}$ , and  $a'$ ,  $\{2\bar{1}\bar{1}0\}$ , which are at opposite ends of the diad axes parallel to the Miller-Bravais axes  $a_1$ ,  $a_2$ ,  $a_3$ , are reported as extremely rare in nature.<sup>7</sup>) The synthetic quartz crystals we studied were of the shape shown in Fig. 2, which is drawn in the orientation of Fig. 1. They were kindly given to us by C. S. Brown of the General

Electric Company Ltd., Wembley, England. The crystals had been grown on  $z$ -cut seed plates [i.e., plates cut parallel to (0001)], from which they had subsequently been severed by a cut parallel to (0001). The crystals had also been trimmed by cuts parallel to  $(1\bar{2}10)$  and  $(\bar{1}2\bar{1}0)$ , and by a cut skimming the upper surface parallel to (0001). However, the last-mentioned cut had fortunately left behind some patches of the unsmooth terminating surface, roughly parallel to (0001), which is a characteristic feature of synthetic quartz crystals grown on  $z$ -plate seeds. (It is interesting to note that this type of seed also forces development of the nonnatural faces  $(1\bar{2}10)$  and  $(\bar{1}2\bar{1}0)$ . These are unsmooth, but unequally so, and have different growth rates, thus demonstrating the structural difference between faces of forms  $a$  and  $a'$ .) The faces  $r$  and  $z$  did not differ much in appearance from their naturally occurring counterparts, except for a greater profusion of growth hillocks than is found on good quality natural specimens. The lower (0001)-cut surface of the crystals was approximately square, about 45 mm in edge length, and the height parallel to the  $c$  axis was about 16 mm. The growth conditions were as follows: growth solution, sodium carbonate, molality 1.7; pressure in the range 0.8 to 1 kbar; temperature about 350°C. The growth rate measured in the  $c$ -axis direction was about 0.5 mm per day; on each side of the seed.

To prepare specimens suitable for mounting on the x-ray goniometer, a number of slices, each about 1 mm thick, were cut so as to sample the imperfection content at various locations in the crystal. The specimens included a slice parallel to  $(10\bar{1}1)$  containing the final growth surface of the largest  $r$  face, another slice parallel to  $r$  but located about 2 mm below the final surface, slices parallel to (0001) taken from the lowest part of the crystal, i.e., closest to the seed, and also from the top of the crystal so as to contain the final, rough, surface parallel to (0001), and slices parallel to  $(1\bar{2}10)$  taken from the center and outer parts of the crystal.

Projection topographs<sup>8</sup> were taken with  $AgK\alpha$  radiation, and recorded on Ilford L4 nuclear plates which were processed at 0°C. The rather large size of the specimens, together with the need sometimes to use rather oblique reflections, meant that the photographic plate could not always be placed as close to the specimen as was desirable for obtaining good topographic reso-

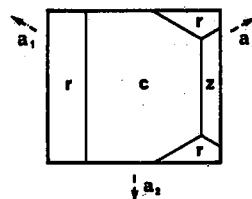


FIG. 2. View of crystal along  $c$  axis, orientation same as Fig. 1. Faces  $r$  and  $z$  are smooth; surface  $c$ , with mean orientation parallel to (0001), is rough.

<sup>6</sup> W. J. Spencer and K. Haruta, *J. Appl. Phys.* **37**, 549 (1966).  
<sup>7</sup> C. Fondel, *Dana's System of Mineralogy* (John Wiley & Sons, Inc., New York, 1962), 7th ed., Vol. III.

<sup>8</sup> A. R. Lang, *Acta Cryst.* **12**, 249 (1959).

FIG. 3. X-ray topograph of slice cut parallel to  $(\bar{1}\bar{2}10)$ , thickness 0.7 mm, width of field 7 mm. Growth direction,  $[0001]$ , is vertical. Reflection  $10\bar{1}0$ ; diffraction vector  $g$  is horizontal.

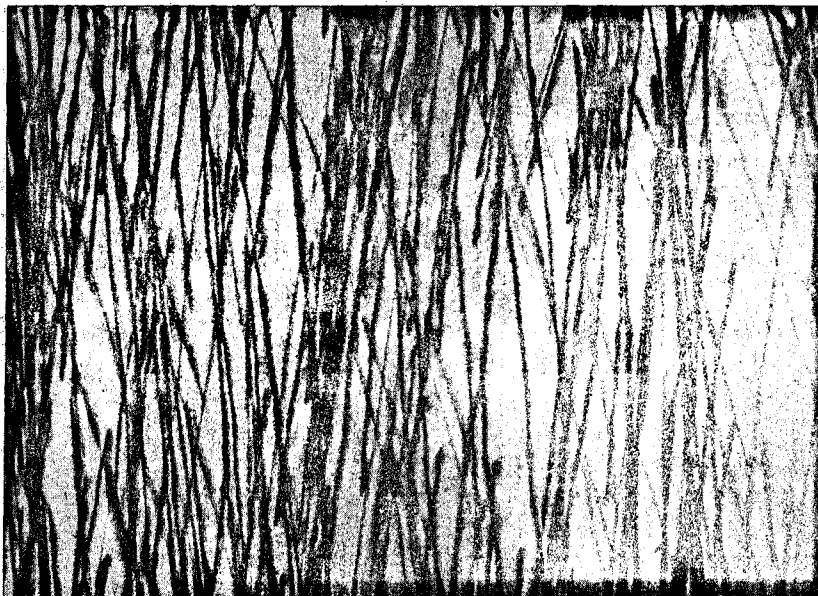


FIG. 4. Topograph of slice cut parallel to  $(10\bar{1}1)$ , thickness 0.7 mm, field width 7 mm, reflection  $\bar{1}011$ , projection of  $c$  axis is vertical.

lution. However, geometric contributions to diffusion of topograph images could generally be kept below 2 to 3  $\mu$ , so that the image widths recorded from dislocations were substantially their natural diffraction widths. Dislocation image width and contrast is discussed further in Sec. 3.4.

### 3. OBSERVATIONS

#### 3.1. Dislocation Configuration

In its typical habit, natural quartz occurs as a hexagonal prism capped by a pyramid consisting of the

major and minor rhombohedral forms plus small facets of rarer forms. The great bulk of the crystal, if not all of it, is formed by growth on the major and minor rhombohedra. A slice cut from the crystal, when examined by x-ray topography, usually discloses quite clearly the division of its area into the several growth sectors corresponding to regions which have grown on different rhombohedral faces. This division is shown by the orientation of growth layers, which commonly produce diffraction contrast, and by growth-sector boundaries which sometimes produce diffraction contrast.<sup>5,9</sup>

<sup>9</sup> A. R. Lang and V. F. Miuscov, *Acta Cryst.* 20, A275 (1966).



FIG. 5. Topograph of slice cut parallel to (0001) containing part of final growth surface. Thickness 0.7 mm, field width 7 mm. Rhombohedral plane reflection, projections of  $g$  and of  $c$  axis are vertical. Dislocations and fault surfaces make fairly small angles with [0001].

It is found, moreover, that it is the local growth direction that controls the direction of grown-in dislocations: departures by more than about  $30^\circ$  from perpendicularity to the local growth face have not been observed. In contrast to natural crystals, the synthetic crystals we have studied have grown entirely in a single direction, that of the  $c$  axis, save for quite thin layers, not more than about 1 mm thick, that have grown on the  $r$  and  $z$  faces. The same rule regarding dislocation line orientation applies as with natural crystals, and apparently more strictly. The great majority of dislocations make not more than  $12^\circ$  with the  $c$  axis. This alignment can be seen in the topograph, Fig. 3. A curious feature is that exact alignment with [0001] is avoided: the distribution of orientations has a maximum on a cone whose axis is [0001] and semi-angle  $10^\circ$ . This characteristic is best seen on topographs of specimen slices cut parallel to (0001), taken with reflections from planes in the [0001] zone having low Bragg angles, such as  $\{10\bar{1}0\}$ .

In the lowest part of the crystal the dislocations are randomly distributed in density, but as growth proceeds in the  $c$  direction a grouping to form cells soon develops. This preferential disposition of dislocations in a polygonal cell boundary network can be seen in Fig. 4 which covers a range of depths from about 5 mm to 10 mm below the upper, terminating surface. The angle of view in this topograph makes about  $30^\circ$  with [0001]. The cell structure reaches its maximum development at the rough final surface whose mean orientation is (0001). Here, as topographs of cuts including this surface show (see Fig. 5), cell boundaries are outlined by stacking-fault-type fringes due to fault surfaces coinciding with these boundaries. The greater concen-

tration of dislocations in or near cell walls is also seen in Fig. 6, which is again of a slice parallel to (0001), but below that shown in Fig. 5, so that the cells are not quite as strongly developed as in Fig. 5.

Figure 6 shows the thin layers which have grown on the  $r$  and  $z$  faces. In contrast to the great bulk of the crystal which has grown in the [0001] direction ( $c$  growth) the layers of  $r$  and  $z$  growth are highly imperfect. Figure 6 reveals two internal surfaces in which severe local strain resides, as shown by their diffraction contrast. The inner one is unsmooth and separates the region of  $c$  growth from the regions of  $r$  growth and  $z$  growth. It is the counterpart of the fault surfaces

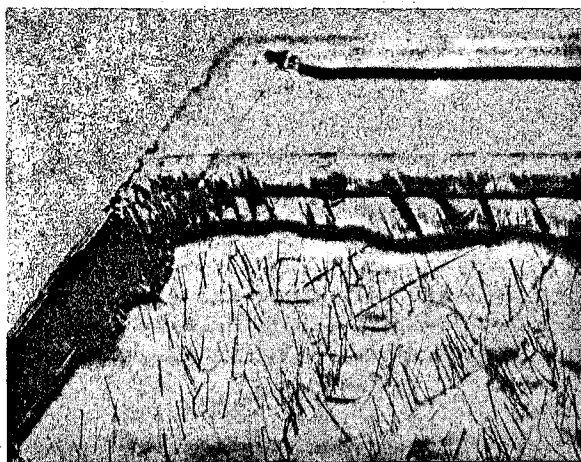


FIG. 6. Topograph,  $10\bar{1}1$  reflection, of slice cut parallel to (0001) showing thin layers of imperfect growth on  $z$  face (above) and on an  $r$  face (left). Growth on  $z$  face reflects weakly because it is misorientated relative to main crystal growth. Field width 8.7 mm.